Supporting Information

A novel bifunctional separator with self-assembled FeOOH/coated g-C_3N_4/KB bilayer in lithium sulfur battery

Yang Wang,[a] Liwen Yang,[a] Yanxiao Chen,[a] Qian Li,[a] Changtao Chen,[a]*

Benhe Zhong,[a] Xiaodong Guo,[ab] Zhenguo Wu,[a] Gongke Wang[c]

[a] College of Chemical Engineering, Sichuan University, Chengdu, 610065, PR China

[b] Institute for Superconducting and Electronic Materials, University of Wollongong, Wollongong, NSW 2522, Australia

[c] School of Materials Science and Engineering, Henan Normal University, Xinxiang, 453007, China

Corresponding Author: Yanxiao Chen

E-mail: yxchen888@163.com

Measurement

Fabrication of S/KB composite and cathode

Ketjen black and elemental sulfur (weight ratio =1:4) were mixed and grounded for 45min. In argon atmosphere, the S/KB composite was successfully fabricated by heating at 155℃ for 12h.The weight ratio of S/KB, acetylene black and PVDF in the S/KB cathode is 8:1:1. The slurry, with NMP, was covered onto the aluminum foil by blade coating and dried for 12h with a temperature of 60℃ in vacuum. Then all the

foils were cut into the same disks. Finally, the sulfur loading of the prepared S/KB cathode is about 1.2-1.5 mg/cm^2.

Assembly of Li-S battery and measurements

Li-S batteries were assembled in Ar atmosphere. All the cells consist of S/KB cathode, metallic lithium, modified separator and commercial electrolytes. Every cell needs 30μL electrolytes contained 1.0M of LiTFISI and 0.1M of $LiNO_3$ in DOL and DME (v:v=50%:50%). And the corresponding E/S ratio is approximately 15:1 (μL/mg). ZenniumIM6 workstation was employed to obtain the electrical impedance spectroscope (EIS). Electrochemical work station (LK 9805) was used to test cyclic voltammetry curves (1.7V-2.8V) at 0.1mV/s. LAND-CT2001A was used for collecting the galvanostatic charging and discharging data (1.7V-2.8V).

Materials characterization

D/Max 2500 PC was used and analyzed to obtain the XRD patterns of modified separators (NSFO, ACSFO, SFO and G-SFO). SPA400 Seiko Instruments was used for checking the morphologies of modified separators (NSFO, PP, SFO and G-SFO). The EDS mapping of separators were all obtained by SEM. TA Instruments, Q600, was used to ensure the sulfur content of S/KB composite. The X-ray photoelectron spectroscopy of SFO and G-SFO separators were analyzed by Kratos Analytical Ltd.

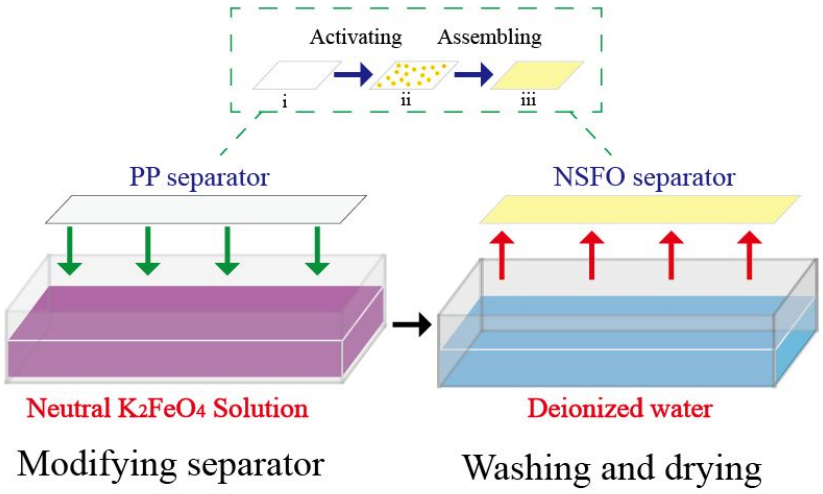

Fig.S1 Schematic illustration of the fabrication process of NSFO modified separator.

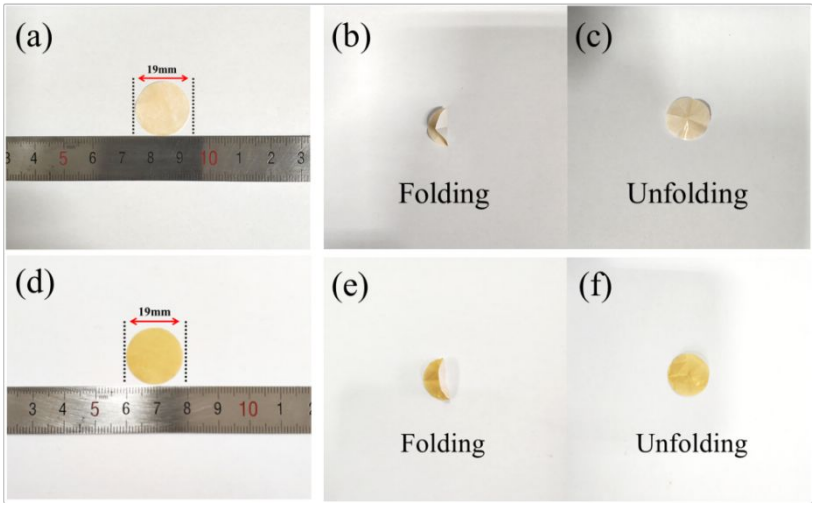

Fig.S2 (a) Digital image of NSFO, (b)-(c) Folding and unfolding test of NSFO, (d) Digital image of SFO, (e)-(f) Folding and unfolding test of SFO.

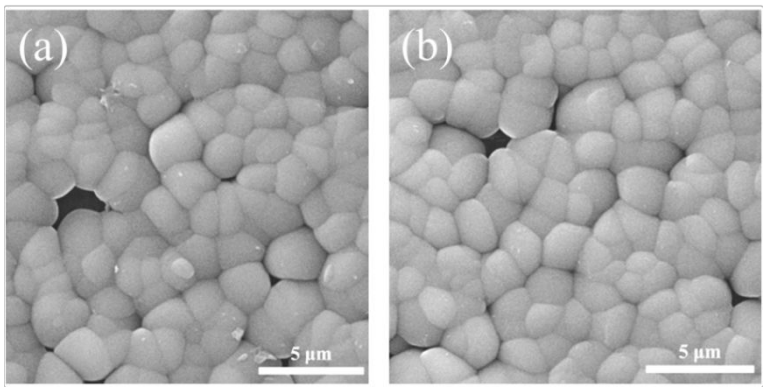

Fig.S3 SEM images of SFO separator after sonication for (a) 5 min and (b) 10 min.

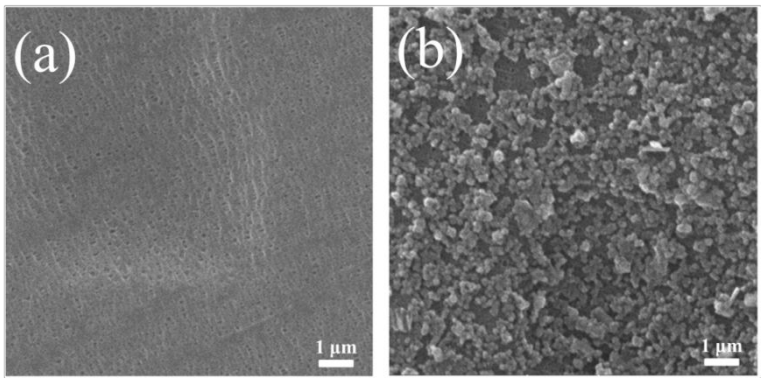

Fig.S4 (a) SEM of pristine PP separator, (b) SEM of NSFO separator

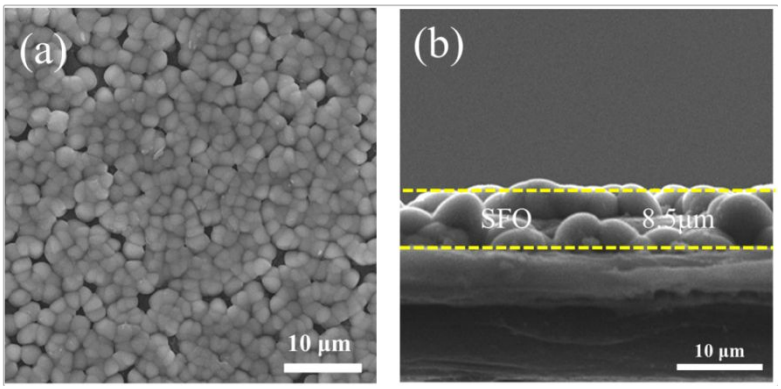

Fig.S5 (a) SEM of SFO separator, (b) Cross-section SEM of SFO separator

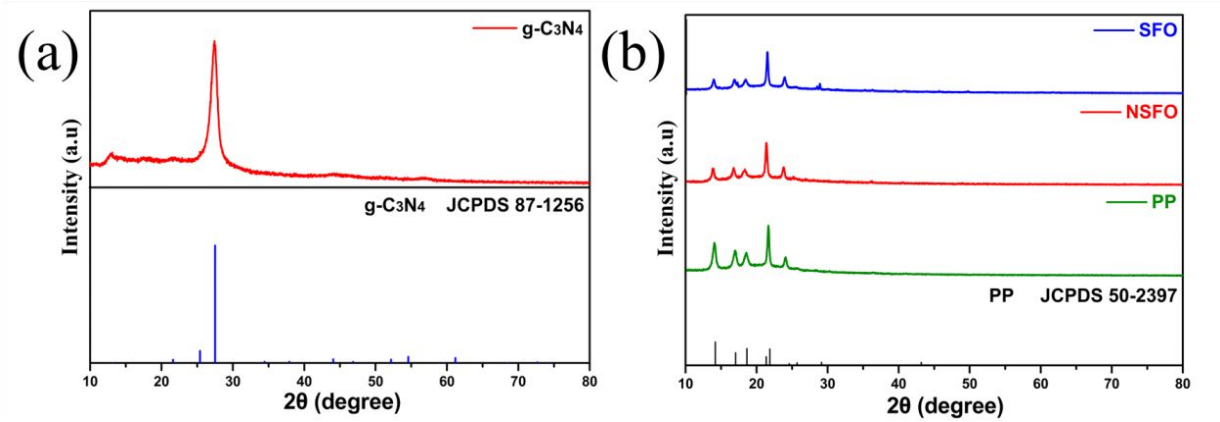

Fig.S6 (a) XRD patterns of g-C_3N_4, (b) XRD patterns of NSFO and SFO separators.

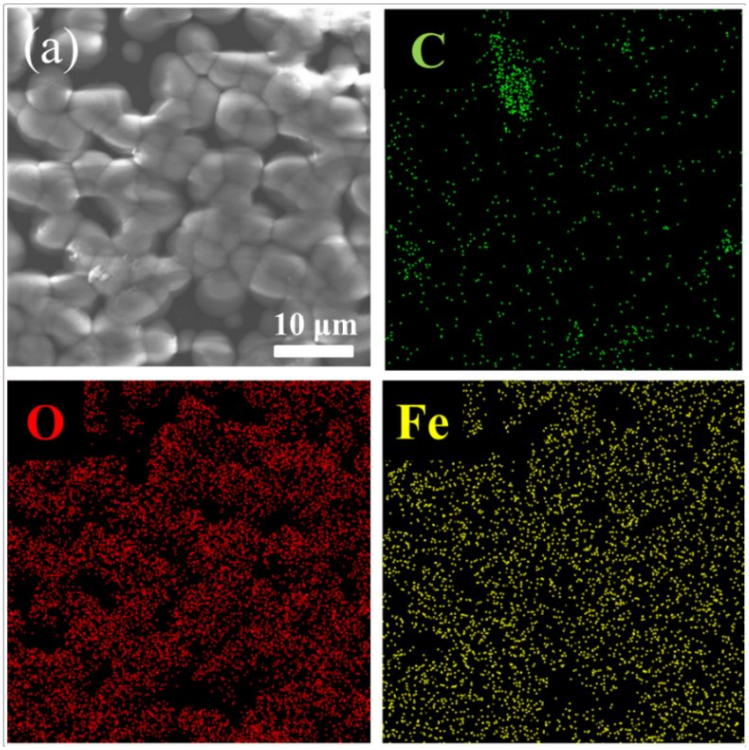

Fig.S7 (a) SEM and the corresponding EDS mapping of SFO separator.

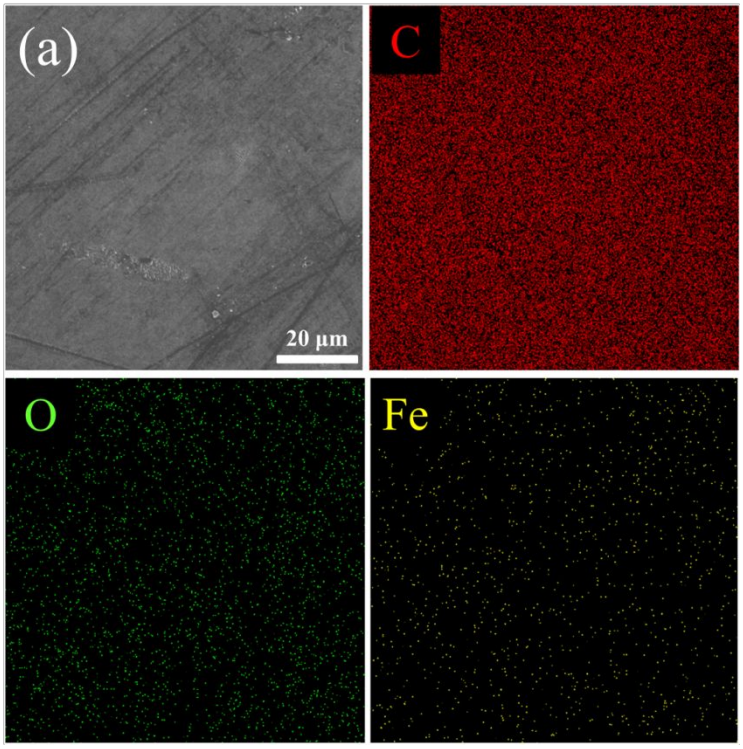

Fig.S8 (a) SEM and the corresponding EDS mapping of SFO separator after etching.

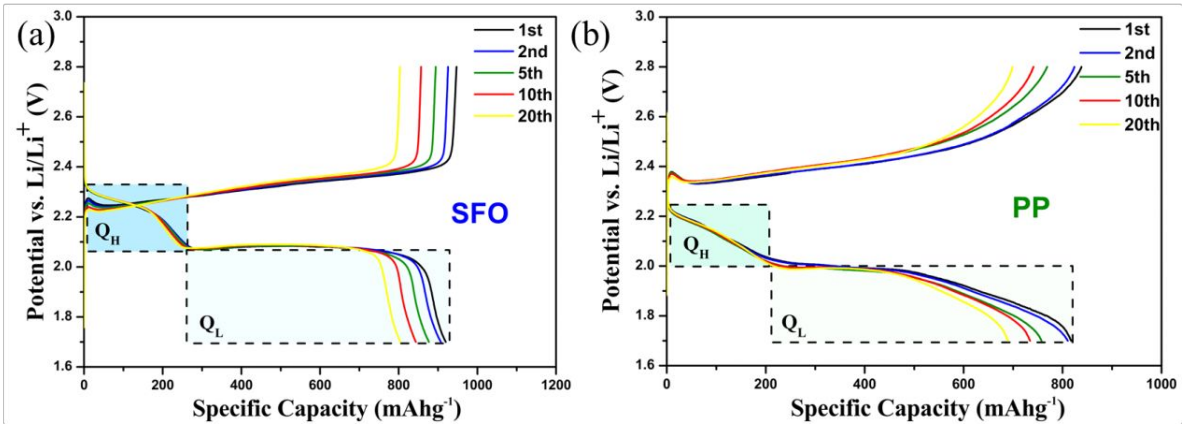

Fig.S9 (a) Charge–discharge curves of the cell with SFO separator at 0.2C, (b) Charge–discharge curves of the cell with PP separator at 0.2C.

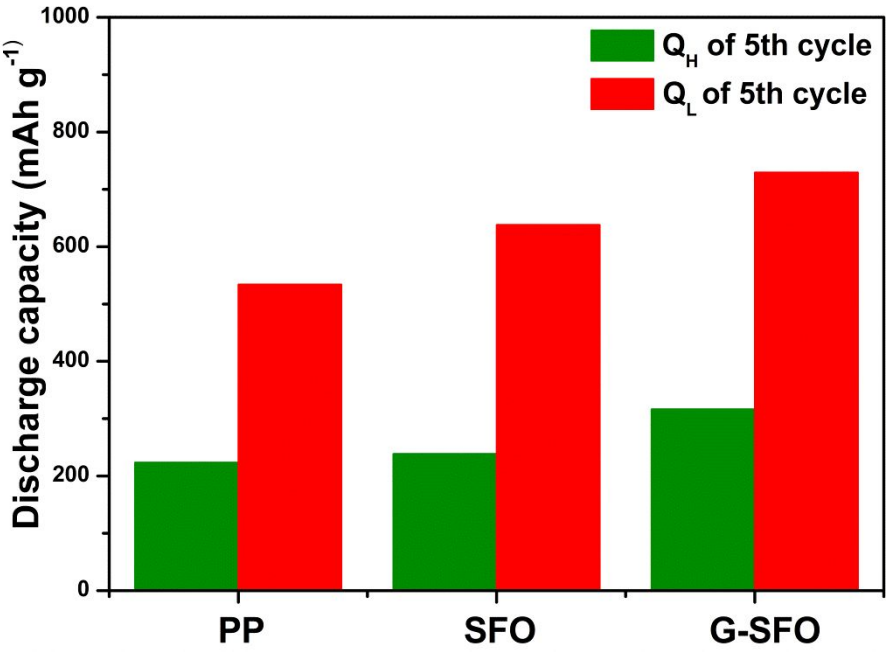

Fig.S10 The Q_H and Q_L values of cells with PP, SFO, G-SFO separators at the 5th cycle at 0.2C.

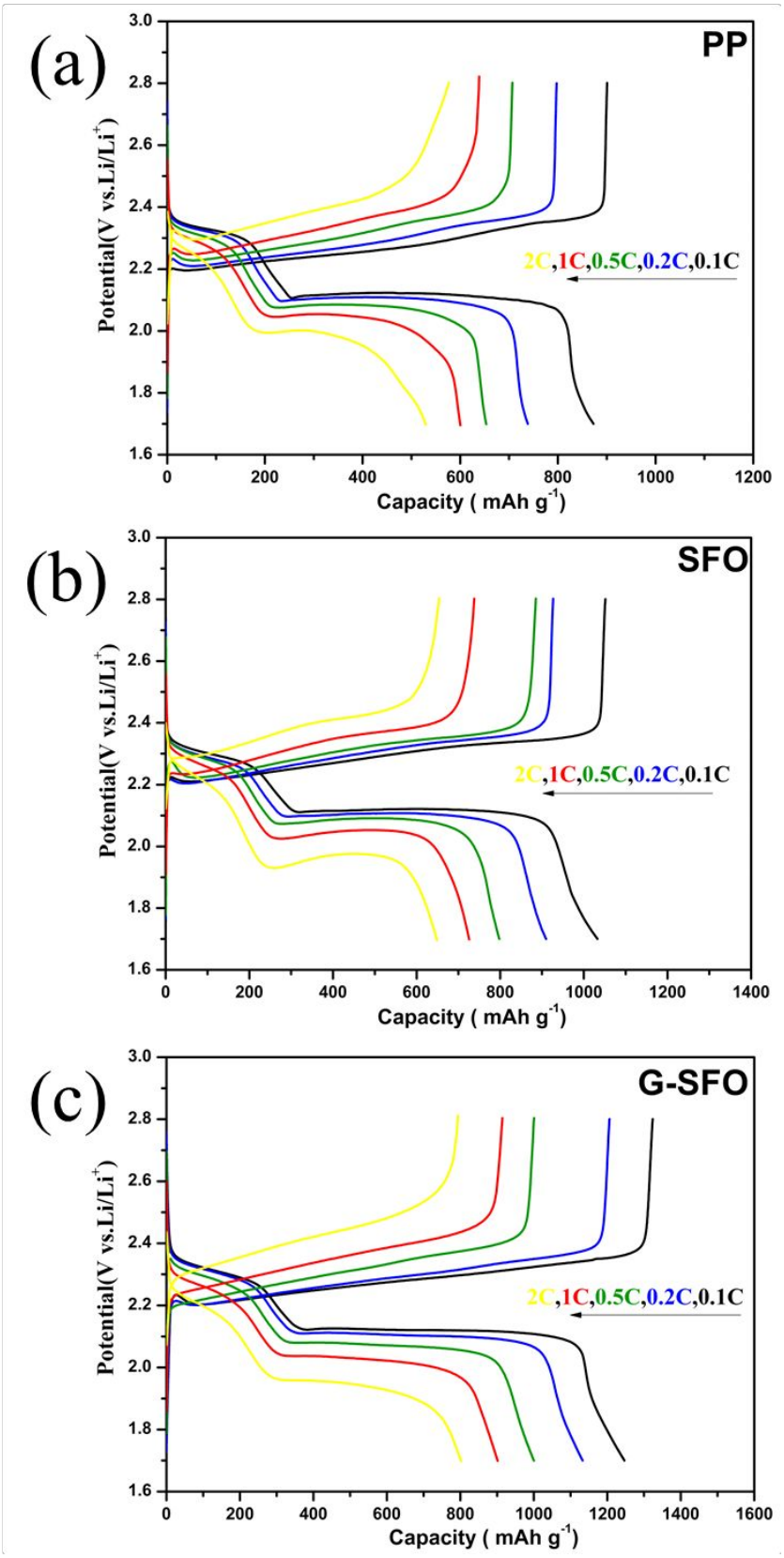

Fig.S11 Charge–discharge curves of the cells with (a) PP separator, (b) SFO separator and (c) G-SFO separator from 0.1C to 2C.

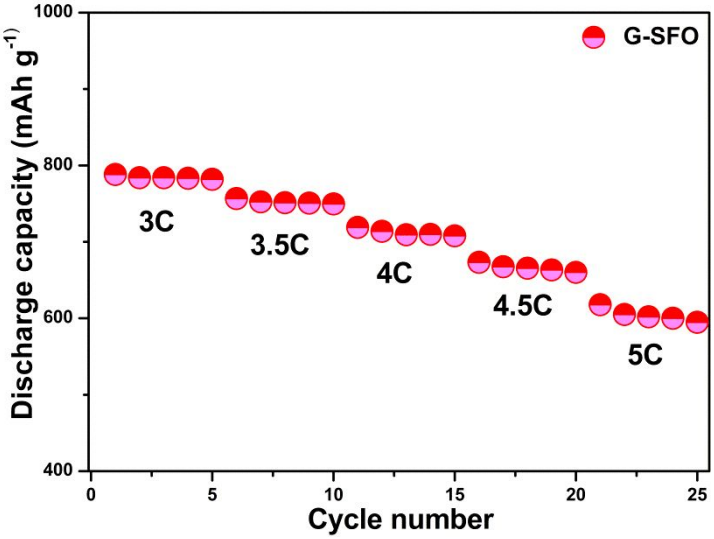

Fig.S12 Rate capacity of the battery with G-SFO separator from 3C to 5C.

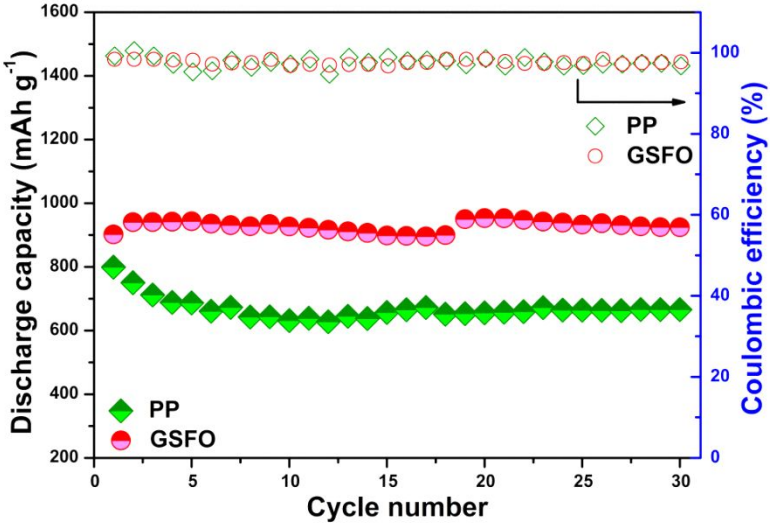

Fig.S13 Cycling performance of the cells with PP and G-SFO separators with high sulfur loading at 0.2 C.

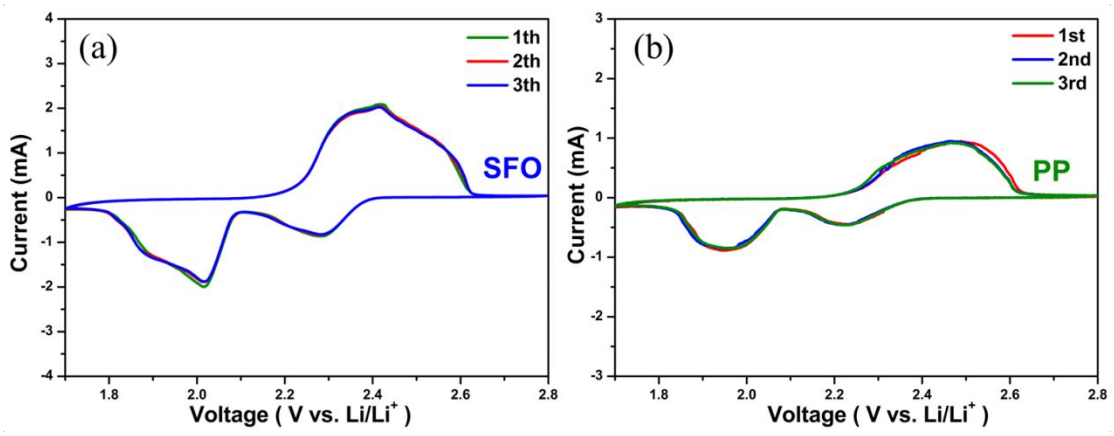

Fig.S14 (a) CV curves of cells with SFO separator, (b) CV curves of cells with PP separator at 0.1mV/s for 3 cycles.

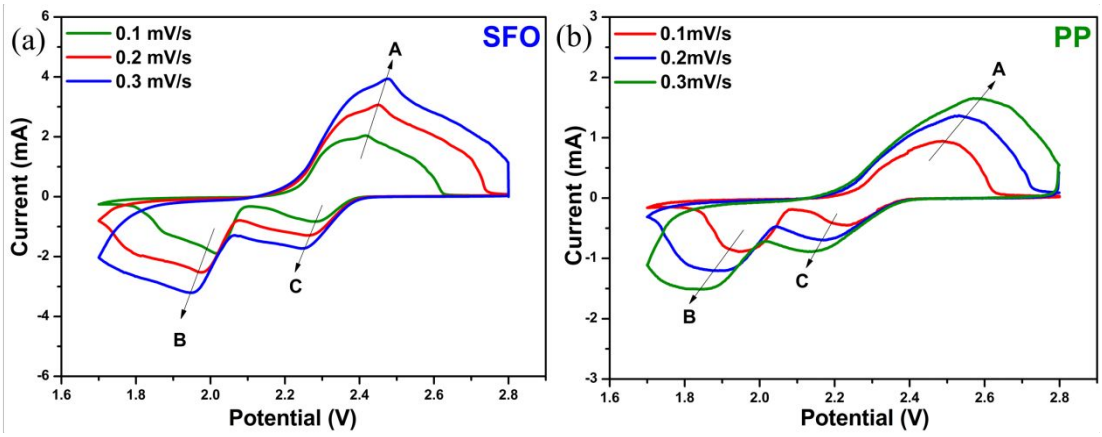

Fig.S15 CV curves of cells with (a) SFO separator and (b) PP separator from 0.1mV/s to 0.3mV/s.

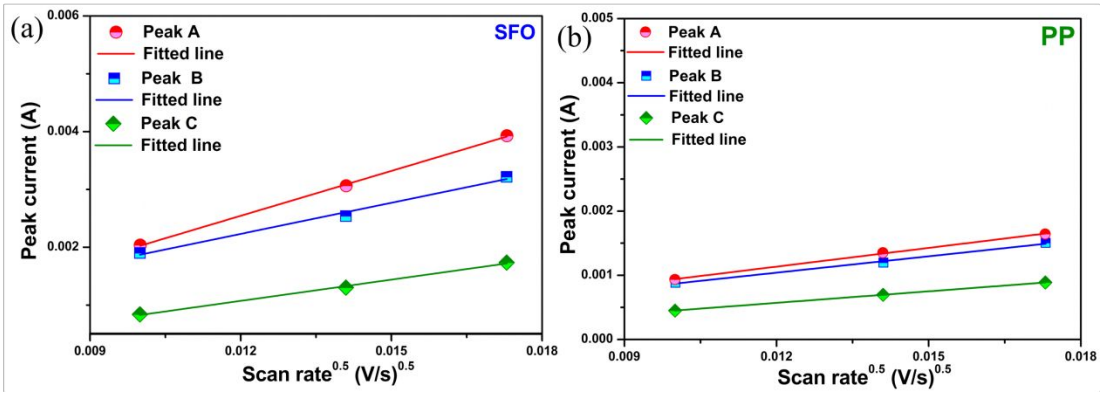

Fig.S16 The linear fits of the peak currents for cells with (a) SFO separator and (b) PP separator.

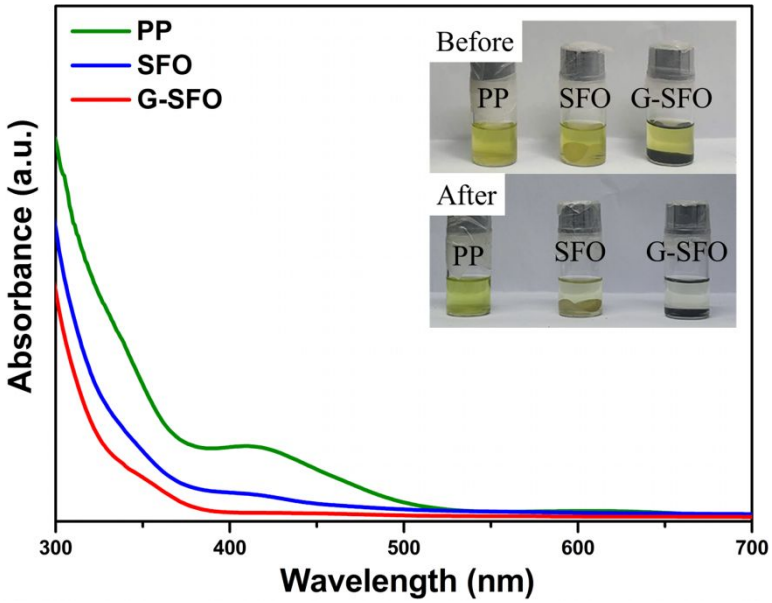

Fig.S17 The adsorption-UV tests of PP, SFO and G-SFO separators.

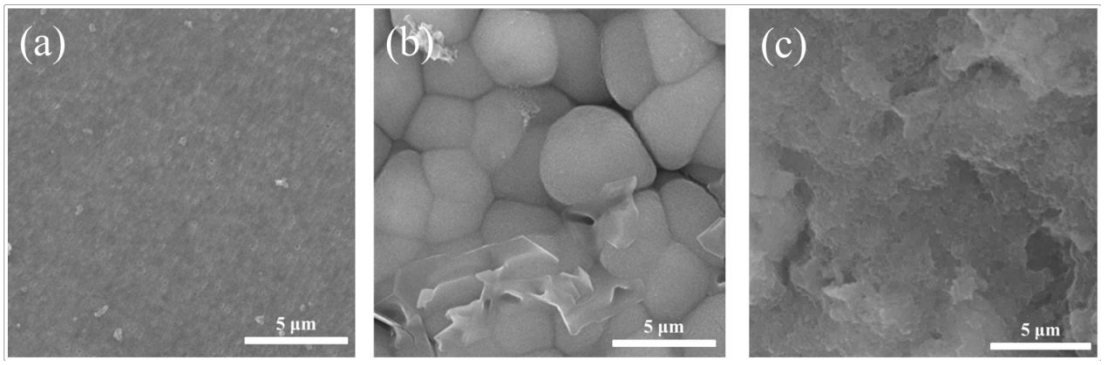

Fig.S18 SEM image of the (a) PP separator, (b) SFO separator and (c) G-SFO separator after cycling.

Table S1.Impedance parameters of different separators

Cell	Impedance	
	$R_s(\Omega)$	$R_{ct}(\Omega)$
PP	3.46	98.09
SFO	3.12	84.35
G-SFO	2.08	50.67

Table S2.Apparent Li^+ diffusion coefficients (D_{Li}^{app}) of cells with different separators

Apparent Li^+ diffusion coefficients			
D_{Li}^{app}	Peak A	Peak B	Peak C
PP	6.92×10^{-9}	5.26×10^{-9}	2.62×10^{-9}
SFO	4.88×10^{-8}	2.35×10^{-8}	1.09×10^{-8}
G-SFO	9.78×10^{-8}	4.32×10^{-8}	2.33×10^{-8}

Table S3. Summary of electrochemical performance of Li-S batteries with different modified separators and interlayers

Materials	Sulfur loading (mg cm^{-2})	Thickness (μm)	Rate Capability (mAh/g)			Cycling Stability			Reference
			0.5C	1C	2C	Rate	Cycles	Decay (per cycle)	
FeOOH/KB/g-C_3N_4	**1.2-1.5**	**12.1**	**1000**	**901**	**802**	**0.5C**	**500**	**0.080%**	***N/A***
						1C	**900**	**0.055%**	***N/A***
Y_2O_3/KB[1]	1.3	12	997	908	846	1C	200	**0.1135%**	Ref S1
ZnO/PPy[2]	0.8	20	718	609	404	0.2C	100	**0.517%**	Ref S2
Cr_2O_3/CNF[3]	1.3-1.6	-	990	960	890	0.2C	260	**0.090%**	Ref S3
Fe_3O_4/PG[4]	0.6-0.9	15	789	673	589	1C	2000	**0.020%**	Ref S4
TiO_2/CNFs[5]	0.8	35	940	740	620	1C	500	**0.051%**	Ref S5
ZnO/Graphene[6]	1.1-1.5	-	1131	895	807	1C	500	**0.093%**	Ref S6
$BaTiO_3$/Rgo/CNFs[7]	1	30	963	852	758	0.3C	200	**0.200%**	Ref S7
$LaLiO_2$[8]	1.1-1.5	-	820	700	600	1C	250	**0.052%**	Ref S8
KB/IR[9]	0.8	20	886	783	653	1C	500	**0.105%**	Ref S9
$Ca(OH)_2$/C[10]	1.2-1.5	4	950	910	830	0.5C	250	**0.112%**	Ref S10

Reference

(1) Wang, S. W.; Qian, X. Y.; Jin, L. N.; Rao, D. W.; Yao, S. S.; Shen, X. Q.; Xiao, K. S.; Qin, S. B. Separator Modified by Y_2O_3 Nanoparticles-Ketjen Black Hybrid and Its Application in Lithium-Sulfur Battery. *Journal of Solid State Electrochemistry* **2017,** *21* (11), 3229-3236, DOI: 10.1007/s10008-017-3649-5.

(2) Yin, F. X.; Ren, J.; Zhang, Y. G.; Tan, T. Z.; Chen, Z. H. A PPy/ZnO Functional Interlayer to Enhance Electrochemical Performance of Lithium/Sulfur Batteries. *Nanoscale Research Letters* **2018,** *13*, DOI: 10.1186/s11671-018-2724-x.

(3) Guan, Y. P.; Liu, X. J.; Akhtar, N.; Wang, A. B.; Wang, W. K.; Zhang, H.; Suntivich, J.; Huang, Y. Q. Cr_2O_3 Nanoparticle Decorated Carbon Nanofibers Derived from Solid LeatherWastes for High Performance Lithium-Sulfur Battery Separator Coating. *Journal of the Electrochemical Society* **2019,** *166* (8), A1671-A1676, DOI: 10.1149/2.1181908jes.

(4) Xiang, Y.; Wang, Z.; Qiu, W.; Guo, Z.; Liu, D.; Qu, D.; Xie, Z.; Tang, H.; Li, J. Interfacing Soluble Polysulfides with a SnO_2 Functionalized Separator: An Efficient Approach for Improving Performance of Li-S Battery. *Journal of Membrane Science* **2018,** *563*, 380-387, DOI: 10.1016/j.memsci.2018.06.004.

(5) Liang, G. M.; Wu, J. X.; Qin, X. Y.; Liu, M.; Li, Q.; He, Y. B.; Kim, J. K.; Li, B. H.; Kang, F. Y. Ultrafine TiO_2 Decorated Carbon Nanofibers as Multifunctional Interlayer for High-Performance Lithium-Sulfur Battery. *ACS Appl. Mater. Interfaces* **2016,** *8* (35), 23105-23113, DOI: 10.1021/acsami.6b07487.

(6) Shi, N. X.; Xi, B. J.; Feng, Z. Y.; Wu, F. F.; Wei, D. H.; Liu, J.; Xiong, S. L. Insight into Different-Microstructured ZnO/Graphene-Functionalized Separators Affecting the Performance of Lithium-Sulfur Batteries. *Journal of Materials Chemistry A* **2019,** *7* (8), 4009-4018, DOI: 10.1039/c8ta12409d.

(7) Zhang, S. Q.; Qin, X. Y.; Liu, Y. M.; Zhang, L. H.; Liu, D. Q.; Xia, Y.; Zhu, H.; Li, B. H.; Kang, F. Y. A Conductive/Ferroelectric Hybrid Interlayer for Highly Improved Trapping of Polysulfides in Lithium-Sulfur Batteries. *Advanced Materials Interfaces* **2019,** *6* (22), DOI: 10.1002/admi.201900984.

(8) Bizuneh, G. G.; Fan, J. M.; Sun, C.; Yuan, X. F.; Xue, F.; Deng, D. R.; Lei, J.; Lin, X. D.; Jia, Y. J.; Yang, J. F.; Yan, H.; Wang, X. Y.; Zheng, M. S.; Dong, Q. F. LaLiO2-Based Multi-Functional Interlayer for Enhanced Performance of Li-S Batteries. *Journal of the Electrochemical Society* **2019,** *166* (2), A68-A73, DOI: 10.1149/2.0271902jes.

(9) Zuo, P. J.; Hua, J. F.; He, M. X.; Zhang, H.; Qian, Z. Y.; Ma, Y. L.; Du, C. Y.; Cheng, X. Q.; Gao, Y. Z.; Yin, G. P. Facilitating the Redox Reaction of Polysulfides by an Electrocatalytic Layer-Modified Separator for Lithium-Sulfur Batteries. *Journal of Materials Chemistry A* **2017,** *5* (22), 10936-10945, DOI: 10.1039/c7ta02245j.

(10) Shao, H. Y.; Huang, B. C.; Liu, N. Q.; Wang, W. K.; Zhang, H.; Wang, A. B.; Wang, F.; Huang, Y. Q. Modified Separators Coated with a $Ca(OH)_2$-Carbon Framework Derived from Crab Shells for Lithium-Sulfur Batteries. *Journal of Materials Chemistry A* **2016,** *4* (42), 16627-16634, DOI: 10.1039/c6ta06828f.